

MoS₂NTs as a novel drug delivery system for oxaliplatin anticancer drug in the presence p and ga impurities in different sites

Mohammed Hamid Neamah¹, Mohammed H. Mohammed^{1,2,3*}

¹Department of Physics, College of Science, University of Thi-Qar, Nassiriya, 64000, Iraq.

²Department of Medical Physics, College of Applied medical Science, Shatrah University, Thi-Qar, 64001, Iraq.

³Department of Physics, College of Science, Southern Illinois University, Carbondale, IL 62901, USA;

mohammed.hamid@utq.edu.iq (M.H.M.).

Abstract: In this study, we are used the (3,2) and (4,2) MoS₂NTs to deliver OX anticancer drug with and without various impurities and sites in different distance between them. The DFT method is used to compute different electronic properties of the complex structures. We found out that the pristine (3,2) and (4,2) MoS₂NTs have semiconductor behavior and the transition of electrons is located at Γ and Z points for (3,2) and (4,2) MoS₂NTs, respectively. The complex structure (OX/(3,2)MoS₂NTs) has a semimetal behavior with direct transition of electrons at Γ point. There are very interesting results by changing the S atom by P or Ga impurities. So, the (OX/p-doped (3,2) MoS₂NTs) structure has a n-type semiconductor behavior when the distance between OX anticancer drug and p-doped (3,2)MoS₂NTs is 1.76 Å compared with other distances. By utilizing Ga impurity, the best results are detected at 1.42 Å and the behavior is became p-type behavior and more stable compared to others. For (OX/(4,2)MoS₂NTs) has metal behavior. By using P impurity at different distance, the behavior is changed from metal to semi-metal with direct transition at Z point. The behavior of this complex structure is became n-type semiconductor at 1.76 Å. For (OX/Ga-doped (4,2)MoS₂NTs) at different distance has a metal behavior, except the 1.82 Å has a n-type semiconductor behavior. The stability of this complex structure became more stable with Ga impurity and the Fermi level is shifted down compared others cases. The stability of all complex structures with Ga impurity is more stable compared with P impurity. In brief, the best substrate of the (3,2) and (4,2) MoS₂NTs can be utilized to career OX anticancer drug when we used Ga impurity compared with P impurity.

Keywords: Adsorption energy, Anticancer drug, DFT method, Electronic band gap,

1. Introduction

The word "cancer" refers to a group of chronic illnesses that vary widely in kind and location, but it is shared by the feature of aberrant cells proliferating uncontrollably. Anticancer drugs also known as antineoplastic drugs are used to treat cancer. There are numerous categories of anticancer medications, such as hormones, alkylating agents, antimetabolites, and natural substances. Platinum drugs continue to be the most effective agents used in cancer treatment among the many alkylating agents [1]. A common chemotherapy medication used to treat colorectal cancer is oxaliplatin, which is based on platinum. It is a member of the alkylating agent family of platinum compounds, which binds covalently to DNA molecules in cancer cells to produce their lethal effects. The transcription and replication of DNA are hampered by this binding, which eventually results in cell death. Due to its proven effectiveness in both adjuvant and metastatic settings, oxaliplatin is a crucial part of many cancer treatment plans [2]. The distinct electronic and structural characteristics of molybdenum disulfide nanotubes (MoS₂NTs) have attracted a lot of interest in the field of drug delivery. Enhancing the

effectiveness and targeted release of this popular chemotherapeutic agent is a promising application of MoS₂ nanotubes for the delivery of oxaliplatin as an anticancer drug. MoS₂NTs are made up of individual molybdenum atom layers nested between two layers of sulfur atoms, creating a hollow core and tubular shape. Their remarkable electronic characteristics, such as a high surface area-to-volume ratio and superior electrical conductivity, result from their special composition. Because of these characteristics, MoS₂NTs are a great choice for drug delivery systems because they effectively encapsulate therapeutic agents and enable their controlled release [3]. There different studied about using nanotubes to deliver this anticancer drugs. The surface of MoS₂NTs contains from sulfur atoms that act as binding sites for the platinum ions in oxaliplatin anticancer drug. Strong drug adsorption and retention within the nanotube structure are facilitated by this interaction, which delays the drug's premature release during circulation in biological systems. Moreover, it is possible to alter the surface's functional groups to improve targeted specificity against tumor cells. It is imperative to evaluate the biocompatibility of MoS₂ nanotubes in order to determine their suitability as drug carriers against cancer. These nanomaterial's effectively inhibit the growth of cancer cells while exhibiting low cytotoxicity towards normal cells, according to in vitro studies. Drug release studies have also shown sustained drug release over an extended period of time with controlled release profiles. These results demonstrate the potential of MoS₂ nanotubes as effective and secure drug delivery vehicles [4]. Zinc oxide nanosheet is utilized to deliver (5-FU, 6-MP, GB, and CP) anticancer drugs. So, they found out that all these complex structures have semiconductor behavior, except, 6-MP/ZnONS has n-type semiconductor behavior. Also, these complex structures have chemisorption, but the 5-FU/ZnONS has physisorption. In additionally, these complex structure are more stable and lower reactive compared with pristine ZnONS [5]. Rezvani et al. utilized the single wall carbon nanotubes (SWCNTs) to deliver oxaliplatin anticancer drug by using van der Waals density functional theory (vdW-DF). They detected that the vdW-DF mostly donate to the binding of selected oxaliplatin anticancer drug and SWCNTs. They noticed that there is not important hybridization among the individual orbital takes place. But there is a small interaction got according to the binding energy [6]. The bilayer of the MoS₂, WS₂, MoSe₂, and WSe₂ nanosheet are utilized to carrier β-lapachone (β-lap) by using DFT method. They found out that these complex structures have become more stable and lower reactive. Also, they detected that there is a higher interaction between the substrate and anticancer drug. There is greater capability to transfer electrons [7]. In this study, we will utilize the MoS₂NTs as a carrier to the oxaliplatin anticancer drug by DFT method due to this tube has a large surface area, adjustable porosity, biocompatibility, exceptional mechanical strength, and chemical [8]. So, we will compute different electronic properties, such as electronic band structure, total energy, and etc with and without (P or Ga impurities) in various locations.

2. Computational Detail

To study how the Oxaliplatin molecule interacts with P/MoSNTs as a drug delivery device, the calculations-based density functional theory with Beck's three-parameter hybrid method utilizing correlation functional of Lee, Yang, Parr (B3LYP) level has been achieved. All geometry fulloptimization has been applied with a hybrid density functional B3LYP/3-21G* basis set [9]. The results were obtained by utilizing the Gaussian 09W and Gauss View 6.0.16 molecular visualization software package. After that, we looked at the molecules' electronic properties, including their electronic band gap (E_{gap}), total energy (E_T), and Fermi energy level (E_{Fl}). The highest-occupied molecular orbital (E_{HOMO}) and lowest-unoccupied molecular orbital (E_{LUMO}) energies were also examined. The following relationships were used to compute the electronic band gap and Fermi level energy [10-16] :

$$E_{gap} = E_{LUMO} - E_{HOMO} \quad (1)$$

$$E_{Fl} = (E_{HOMO} - E_{LUMO}) / 2 \quad (2)$$

According to the DFT method and Koopmans' theorem, we studied the reactivity of these anticancer drugs on the substrate (MoS₂NTs) via computing the next parameters [17-19]:

$$I_P = -E_{HOMO} \quad (3)$$

$$E_A = -E_{LUMO} \quad (4)$$

$$H = (I_P - E_A)/2 \quad (5)$$

$$S = \frac{1}{2H} \quad (6)$$

$$\mu = (I_P + E_A)/2 \quad (7)$$

Where I_P, E_A, H, S, μ , are indicated the ionization potential, electron affinity, chemical hardness, chemical softness, chemical potential, consecutively. After that, we investigated that how can utilize the MoSNTs structure to carry these anticancer drugs by putting this anticancer drug upon the slab of the MoS₂NTs [20]

3. Results and Discussions

3.1. The Electronic Properties of the (OX/ Pristine and N-Doped (3,2) MoS₂NTs).

First of all, we optimized the pristine (3,2) and (4,2) MoS₂NTs by utilizing the DFT method. We found out that these tubes have semiconductor behavior with direct transition of electrons from valence to conduction bands at Γ point, as displayed in Figure 1. Also, the bond length between Mo and S atoms is 2.41 Å. All these results are in agreement with previous references [7, 21-24]. The electronic band structure of the pristine (3,2) and (4,2) MoS₂NTs is displayed in Figure 2. We discovered that the (3,2) MoS₂NTs nanotubes has a semiconductor behavior with electronic band gap is 0.128 eV, which is very comfortable with previous study [25]. So, there is direct transition of electrons from valence to conduction bands at Γ point (pointed out in Fig.2). However, the (4,2) MoS₂NTs has a semimetal behavior due to it has 0.072 eV electronic band gap with direct transition of electrons at Z point, as represented in Figure 2.

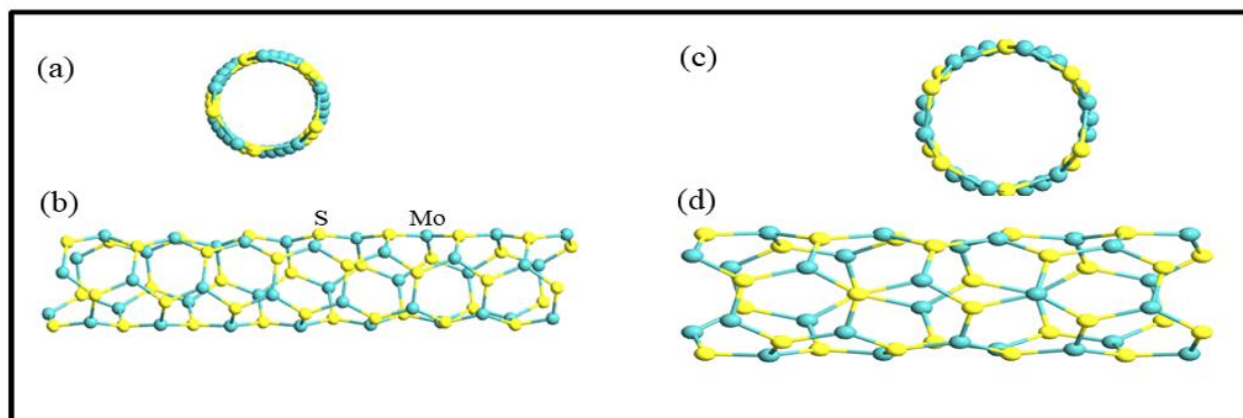


Figure 1.

Optimization structure of the pristine (3,2) MoS₂NTs ((a) Top view and (b) Side view) and (4,2) MoS₂NTs ((c) Top view and (d) Side view)).

After that we computed the electronic properties of the complex structure (OX/pristine (3,2) MoS₂NTs). By optimization this complex structure, the distance between the OX anticancer drug and pristine (3,2) MoS₂NTs became 1.80 Å (see Fig. 3(a)). In additionally, we detected that the behavior is changed from semiconductor to semimetal behavior. So, the electronic band gap is reduced from 0.128 eV to 0.0084 eV with direct transition of electrons from valence to conduction bands at Γ point, as displayed in Fig. 3 (b) and summarized in Table 1. So, we discovered very interesting result when we replaced S atom by P atom (see Fig. 4(a and b), which is connected with OX anticancer drug. So, the

behavior is became semiconductor with direct electron transition at z point, as pointed out in Figure 4 (c). The electronic band gap is increased compared with previous case. This complex structure became more stable and lower reactive due to the total energy is increased compared with previous case, as displayed in Table 1. By increasing the distance between the OX anticancer drug and p-doped MoS₂NTs, the electronic band gap and total energy are increased compared with OX/pristine (3,2) MoS₂NTs, as shown in Fig. 5 and summarized in Table 1. The Fermi level is shifted down, as displayed in Table 1. Also, there are exact fascinating result when we changed the P atom by Ga atom (see Fig.6). So, the behavior is changed from n-type to p-type semiconductor, as revealed in Fig. 7. The electronic band gap and total energy of the OX/Ga-doped MoS₂NTs are increased, excepted the Fermi level energy is shifted up compared with previous cases, as represented in Table 1.

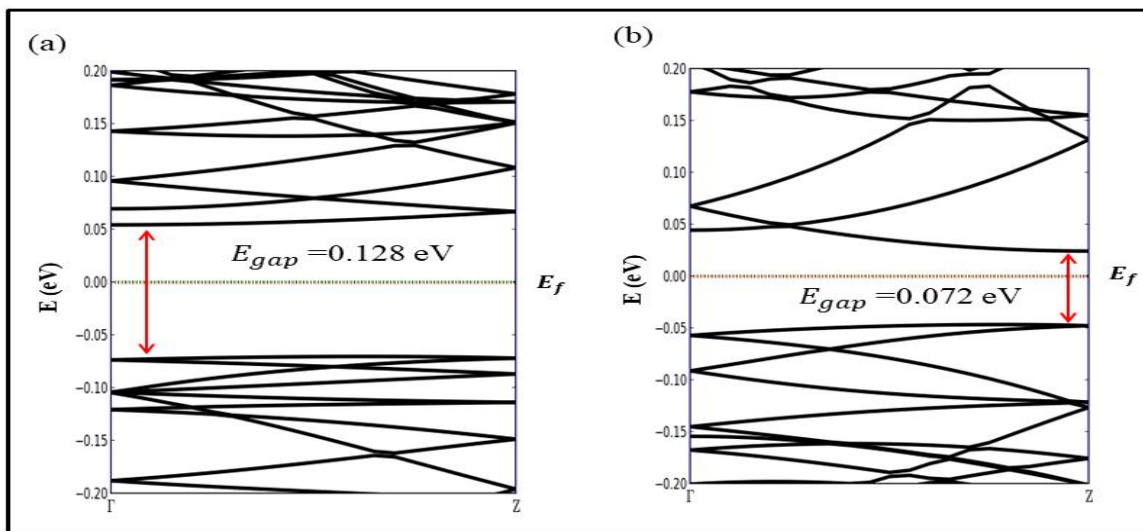


Figure 2.
The electronic band structure of the pristine (3,2)MoS₂NTs (a) and (4,2)MoS₂NTs (b).

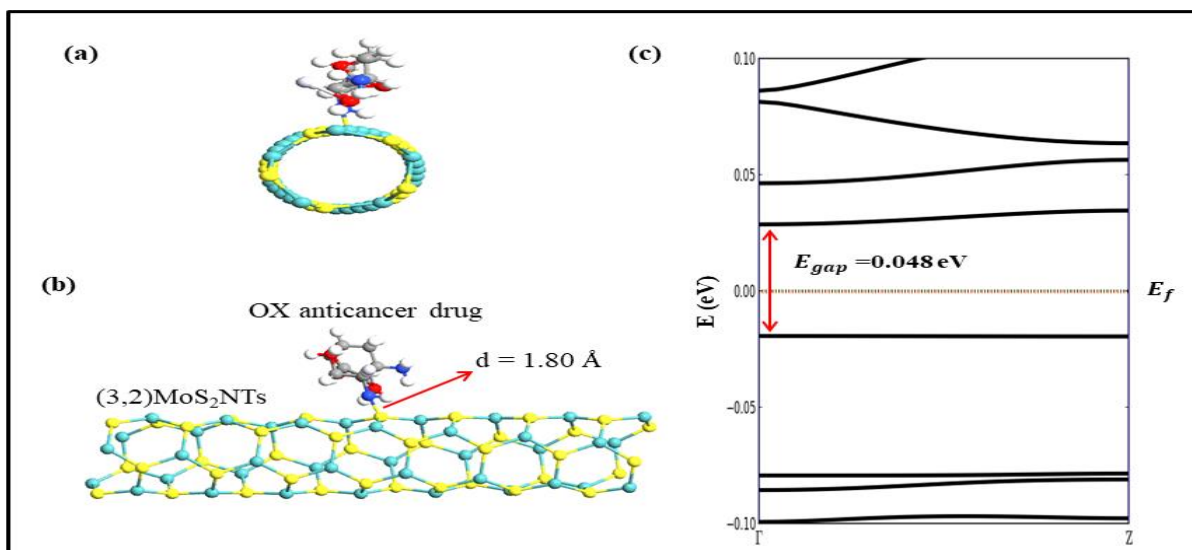


Figure 3.
The complex structure (OX/pristine (3,2) MoS₂NTs); the top and side views (a and b) and the electronic band structure of this complex structure (c).

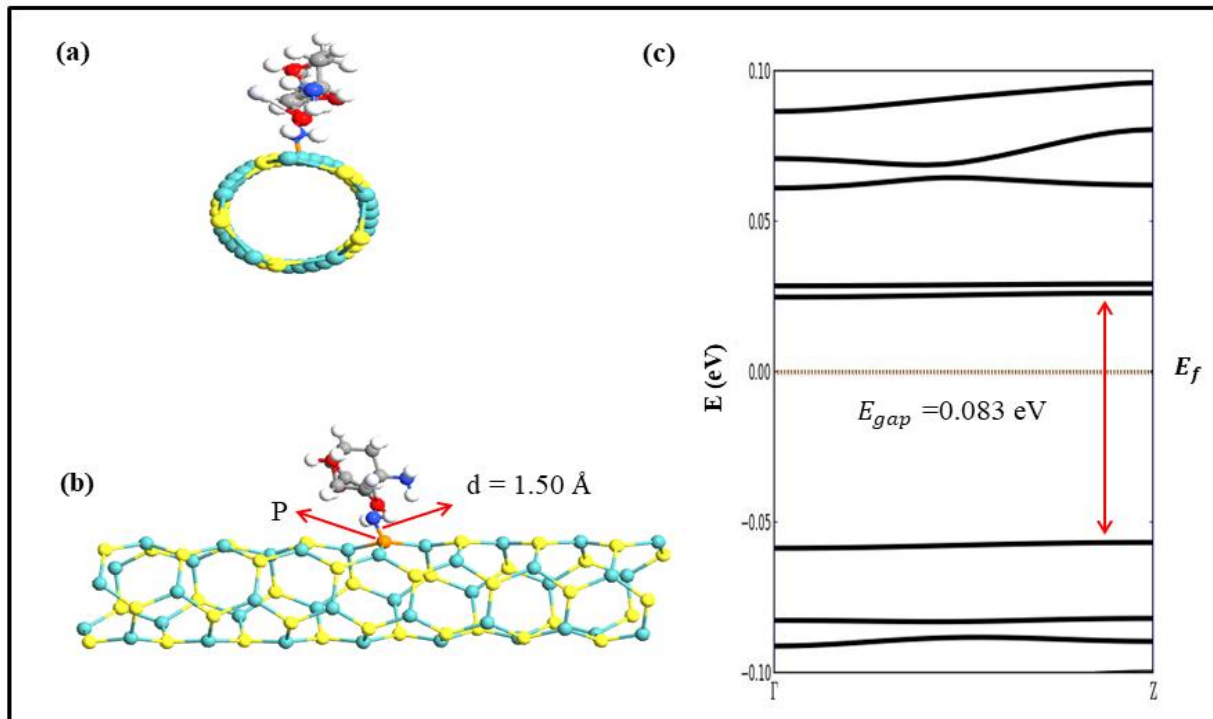


Figure 4.

The complex structure (OX/P-doped (3,2) MoS₂NTs; the top and side views (a and b) at 1.50 Å and the electronic band structure of this complex structure (c).

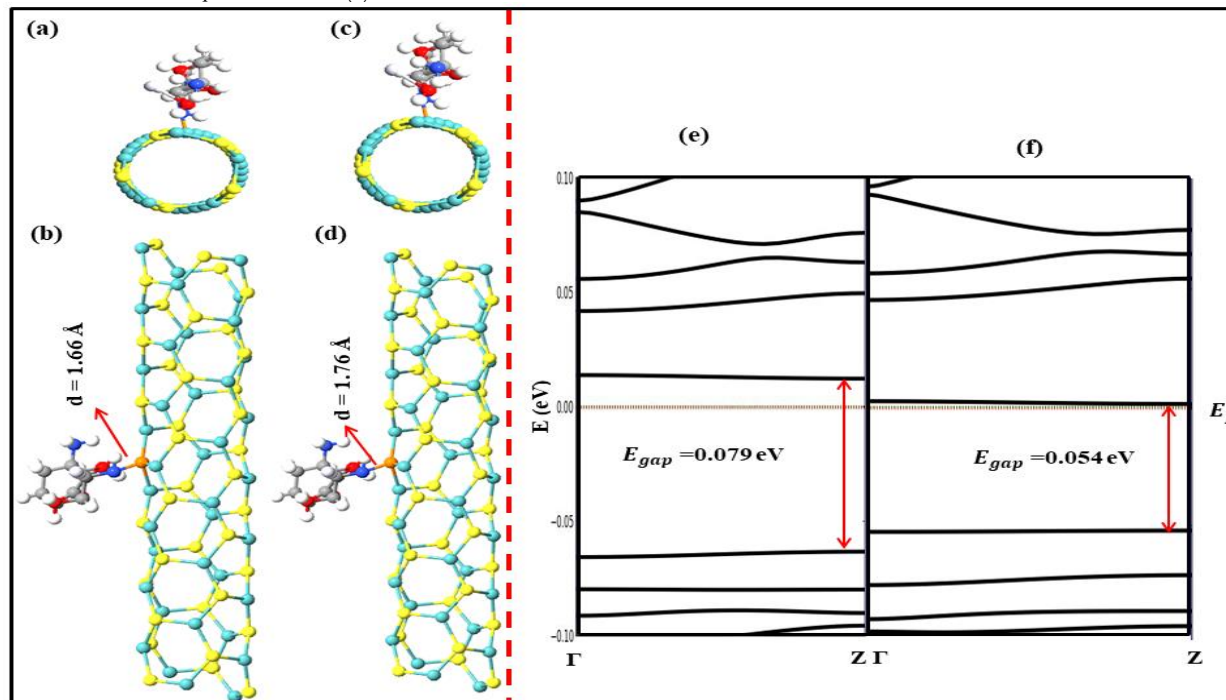


Figure 5.

The complex structure (OX/P-doped (3,2)MoS₂NTs; the top and side views (a and b) and electronic band structure (e) at 1.66 Å and (Top and side views (c and d) and electronic band structure (f) at 1.76 Å), respectively.

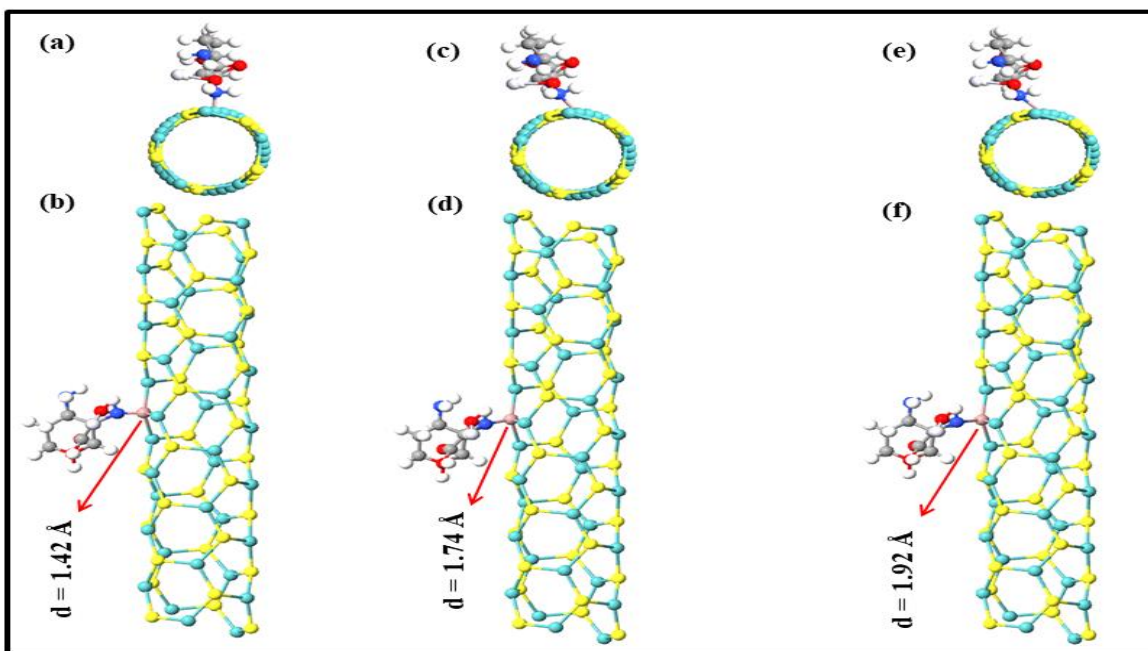


Figure 6. The complex structure (OX/Ga-doped (3,2) MoS₂NTs) in the different distance between tube and OX anticancer drug.

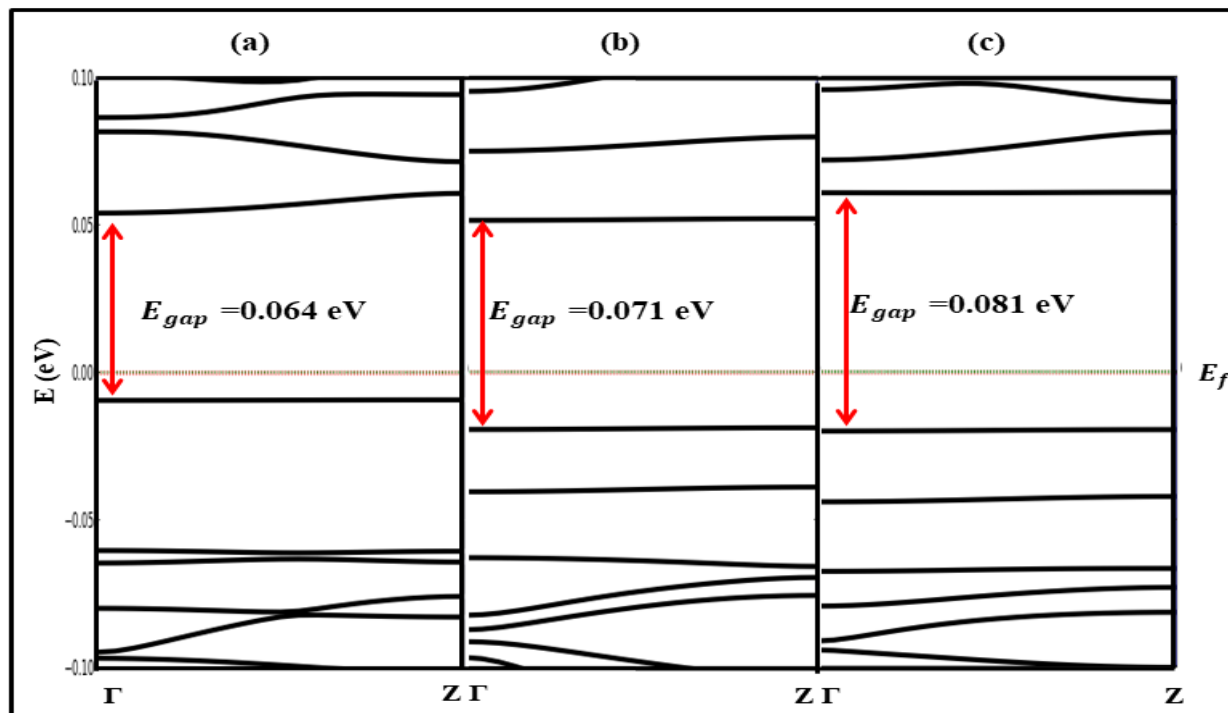


Figure 7. The electronic band structure of the complex structure (OX/P-doped (3,2) MoS₂NTs) in the different distance between the anticancer drug and this tube, (a) at (1.42 Å) (a), (b) at 1.74 Å, and (c) at 1.92 Å.

3.2. The Electronic Properties of the (OX/ Pristine and n-Doped (4,2) MoS₂NTs).

After these results, we are utilized the (4,2) MoS₂NTs. By changing the S atom by P atom (see Fig.8(a and b)), we found out there is not electronic band gap and the behavior is changed from semiconductor to metal when we utilized the distance between OX anticancer drug and Ga-doped MoS₂NTs is 1.80 Å, as represented in Fig. 8 (c). But, when this distance is became (1.50, 1.66, and 1.76) Å, as displayed in Fig. 9 (a and b) the electronic band gap is (0.060, 0.052, and 0.047) eV, correspondingly. Also, the behavior of this complex structure is n-type with these distance, as displayed in Fig. 9 (c and d). In these distance, the total energy is increased and the Fermi level is shifted down comparing with OX/pristine (4,2) MoS₂NTs, as shown in Table 1.

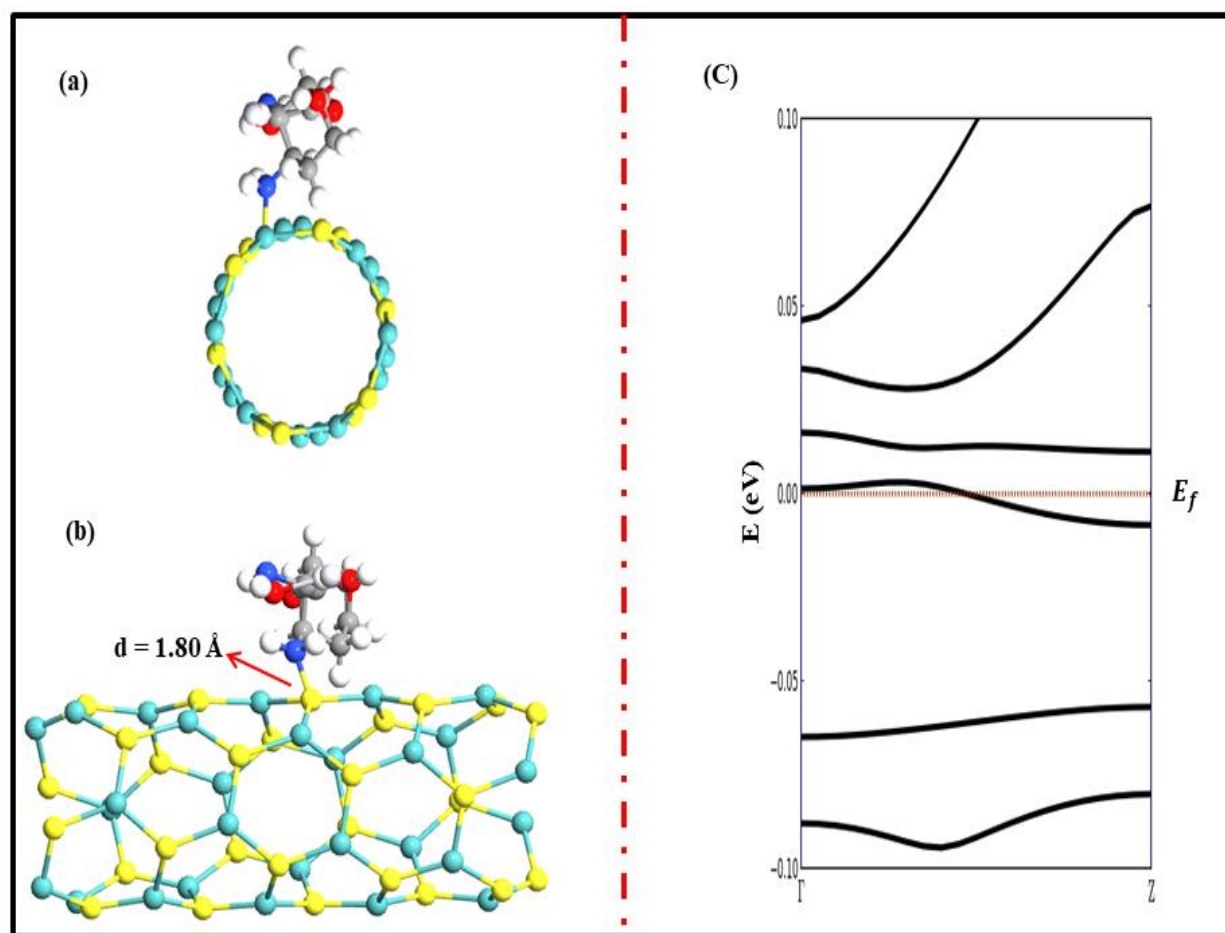


Figure 8.

The complex structure (OX/ (4,2)MoS₂NTs) ; the top and side views (a and b) at 1.80 Å and the electronic band structure of this complex structure (c).

Figure 10 shows the S atom is replaced by Ga atom in various distances. The results shown that the behavior is changed from n-type to metal when we changed the distance between the OX anticancer drug and Ga-doped (4,2)MoS₂NTs compared with previous cases, as shown in Fig. 11 (a and b), excepted the 1.82 Å has a n-type semiconductor, as shown in Fig. 11 (c). Fermi level is shifted down and the stability increased due to the total energy increased compared with previous cases, as summarized in Table 1.

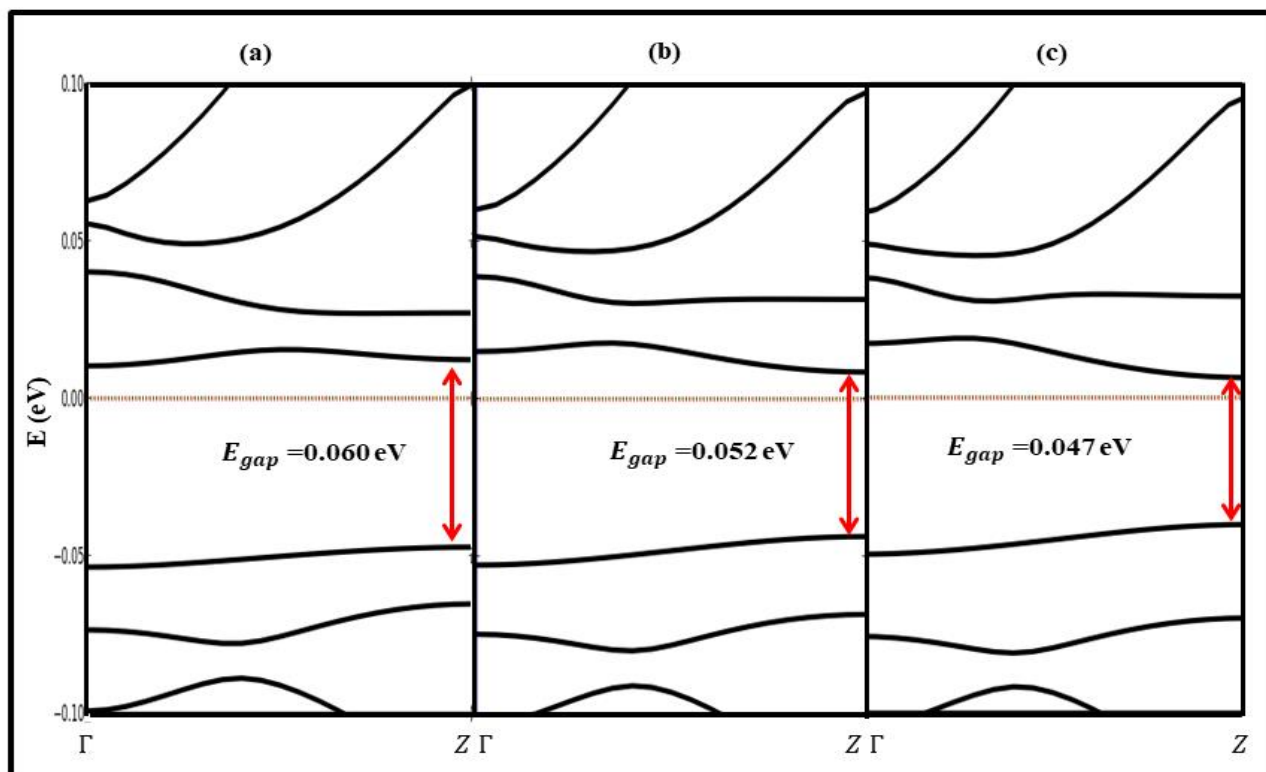


Figure 9.

The electronic band structure of the complex structure (OX/P-doped (4,2) MoS₂NTs) in the different distance between the anticancer drug and this tube, (a) at (1.50 Å) (a), (b) at 1.66 Å, and (c) at 1.76 Å.

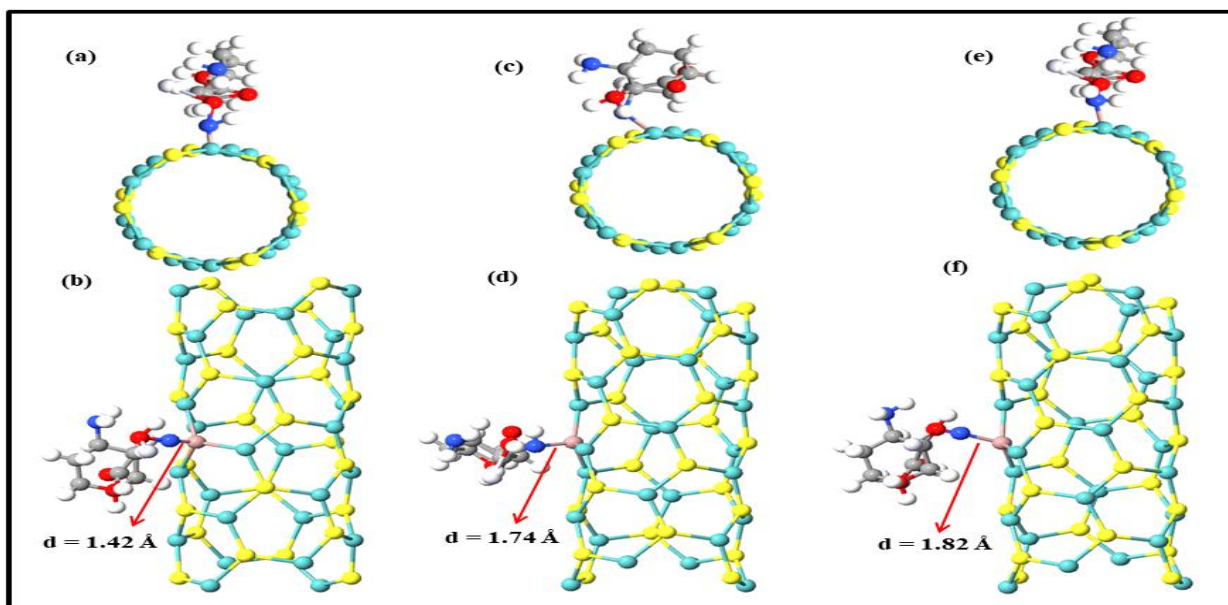


Figure 10.

The complex structure (OX/ (4,2)MoS₂NTs) in the different distance between tube and OX anticancer drug; the top and side views (a and b) at 1.42 Å, the top and side views (c and d) at 1.74 Å, and the top and side views (e and f) at 1.82 Å.

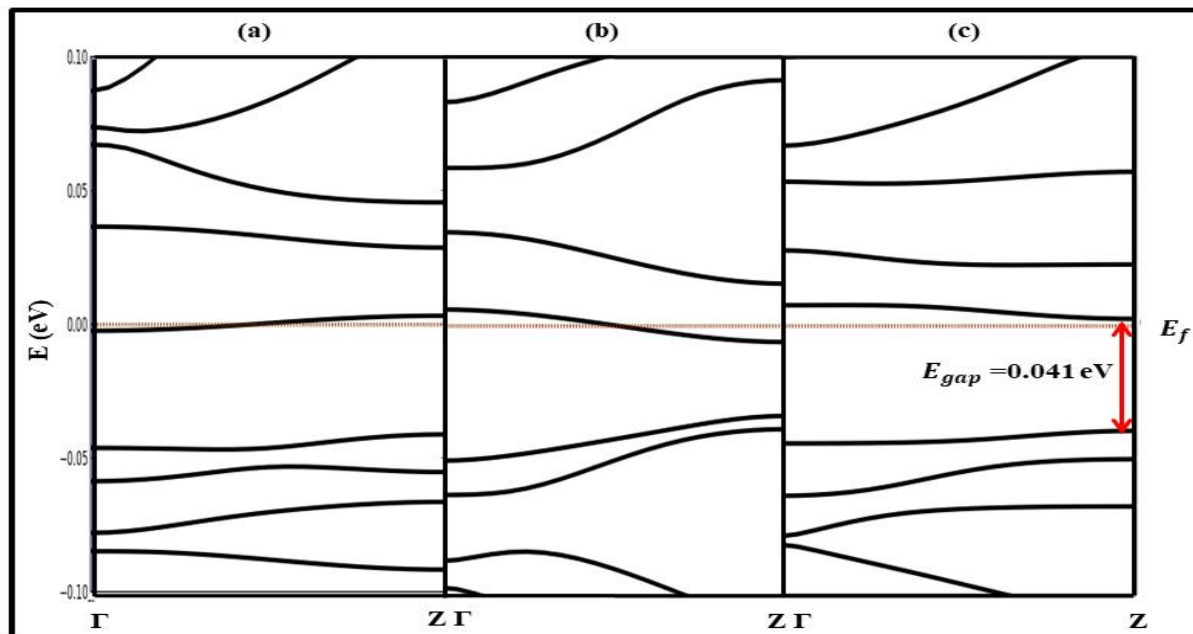


Figure 11.

The electronic band structure of the complex structure (OX/Ga-doped (4,2)MoS₂NTs) in the different distance between the anticancer drug and this tube, (a) at (1.42 Å) (a), (b) at 1.74 Å, and (c) at 1.82 Å.

Table 1.

Some electronic properties of the pristine and complex structures; d , E_{gap} , E_T , E_f and are denoted the distance between tube and OX anticancer drug, electronic band gap, total energy, and Fermi level energy, respectively.

System	d (Å)	E_{gap} (eV)	E_T (eV)	E_f (eV)
(3,2) MoS ₂ NTs	-	0.128	-3084.739	-3.195
OX/Pristine (3,2) MoS ₂ NTs	1.80	0.048	-1832.377	-3.154
OX/P-doped (3,2) MoS ₂ NTs	1.50	0.083	-1886.179	-3.158
OX/P-doped (3,2) MoS ₂ NTs	1.66	0.079	-1870.032	-3.160
OX/P-doped (3,2) MoS ₂ NTs	1.76	0.054	-1857.697	-3.164
OX/Ga-doped (3,2) MoS ₂ NTs	1.42	0.064	-2017.826	-3.167
OX/Ga-doped (3,2) MoS ₂ NTs	1.74	0.071	-2023.859	-3.158
OX/Ga-doped (3,2) MoS ₂ NTs	1.92	0.081	-1833.614	-3.156
(4,2) MoS ₂ NTs	-	0.072	-22729.037	-3.287
OX/Pristine (4,2) MoS ₂ NTs	1.80	0.049	-628.713	-3.151
OX/P-doped (4,2) MoS ₂ NTs	1.50	0.060	-653.005	-3.174
OX/P-doped (4,2) MoS ₂ NTs	1.66	0.052	-654.860	-3.168
OX/P-doped (4,2) MoS ₂ NTs	1.76	0.047	-654.735	-3.166
OX/Ga-doped (4,2) MoS ₂ NTs	1.42	0.044	-872.458	-3.209
OX/Ga-doped (4,2) MoS ₂ NTs	1.74	0.028	-835.397	-3.221
OX/Ga-doped (4,2) MoS ₂ NTs	1.82	0.041	-837.694	-3.199

3.3. The Global Reactivity of The Complex Structures

Depending on the Koopmans' theorem, we found out there is very small value of the μ of the pristine (3,2) MoS₂NTs, which led to make a lower chemical reactivity. For all complex structures (OX/(p or Ga)-doped (3,2) MoS₂NTs), the μ value is increased comparison with OX/pristine MoS₂NTs, but it is still has a lower reactivity due to there is smaller value of the μ , as represented in Table 2. Also, the

results shown that the pristine (3,2) and (4,2) MoS₂NTs have a smaller value of the I_p , which led to a higher ability to donate the electrons and became cation comparison with complex structures, as displayed in Table 2. The (OX/p-doped (3,2)MoS₂NTs) at 1.66 Å (a distance between OX anticancer drug and (3,2) MoS₂NTs) has a higher value of the I_p , which refers to higher ability to acceptance an electrons and became anion, as demonstrated in Table 2. The pristine (3,2) and (4,2) MoS₂NTs have a higher value of the H comparison with all complex structures, which is referred to lower ability to transfer an electron. Then, they required a higher exaction energy to transfer electrons, as mentioned in Table 2. There is a higher value of the S in the OX/pristine (3,2) MoS₂NTs compared with others structures, which is led to make the distance between the valence and conduction very small. So, this result is very comfortable with result is shown in Fig.3 (c) . However, it is increased by suing various impurities and distance between the tube and OX anticancer drug, as displayed in Table 2. Our finding shown that there is a great interaction between the OX anticancer drug and pristine or P or Ga-doped MoS₂NTs because of the ω has a higher value in the complex structure comparison with pristine MoS₂NTs, as shown in Table 2.

Table 2.

The global chemical indexes of the pristine and complex structures; I_p , E_A , H , S , μ , and ω are denoted the ionization potential, electron affinity, chemical hardness, chemical softness, electrophilicity index, and electronegativity (All these properties in the eV unit).

System (Drug with tube)	d (Å)	I_p	E_A	H	S	μ
(3,2) MoS ₂ NTs	-	0.066	-0.058	0.062	8.065	0.004
OX/Pristine (3,2) MoS ₂ NTs	1.80	0.017	-0.028	0.023	21.740	-0.006
OX/P-doped (3,2) MoS ₂ NTs	1.50	0.056	-0.026	0.041	12.195	0.015
OX/P-doped (3,2) MoS ₂ NTs	1.66	0.062	-0.013	0.038	13.158	0.025
OX/P-doped (3,2) MoS ₂ NTs	1.76	0.050	-0.001	0.026	19.231	0.025
OX/Ga-doped (3,2) MoS ₂ NTs	1.42	0.008	-0.054	0.031	16.129	-0.023
OX/Ga-doped (3,2) MoS ₂ NTs	1.74	0.019	-0.053	0.036	13.882	0.017
OX/Ga-doped (3,2) MoS ₂ NTs	1.92	0.019	-0.061	0.040	12.500	0.021
(4,2) MoS ₂ NTs	-	0.071	-0.055	0.063	7.937	-0.019
OX/Pristine (4,2) MoS ₂ NTs	1.80	0.058	0.008	0.025	20.00	0.033
OX/P-doped (4,2) MoS ₂ NTs	1.50	0.052	-0.011	0.032	15.625	0.021
OX/P-doped (4,2) MoS ₂ NTs	1.66	0.043	-0.009	0.026	19.231	0.017
OX/P-doped (4,2) MoS ₂ NTs	1.76	0.040	-0.006	0.023	21.739	0.017
OX/Ga-doped (4,2) MoS ₂ NTs	1.42	-0.046	-0.002	-0.022	-22.727	-0.024
OX/Ga-doped (4,2) MoS ₂ NTs	1.74	-0.032	-0.006	-0.015	-34.483	-0.019
OX/Ga-doped (4,2) MoS ₂ NTs	1.82	0.038	-0.003	0.021	23.819	0.018

4. Conclusion

In this study, the (3,2) and (4,2) MoS₂NTs are utilized to carry OX anticancer drug with and without various impurities and sites in different distance between them. Different electronic properties of these complex structures are computed by using DFT method. Results shown that the pristine (3,2) and (4,2) MoS₂NTs have semiconductor behavior with direct transition of electrons at Γ and Z points for (3,2) and (4,2) MoS₂NTs, individually. So, the (OX/(3,2)MoS₂NTs) structure has a semimetal behavior with direct transition of electrons at Γ point. By replacing S atom with P or Ga impurities in different distances and locations. There are very exciting results. The (OX/p-doped (3,2) MoS₂NTs) structure has a n-type semiconductor behavior when the distance between OX anticancer drug and p-doped (3,2)MoS₂NTs is 1.76 Å compared with other distances. For Ga impurity, the greatest results are discovered at 1.42 Å and the behavior is became p-type behavior and more stable compared to others. For (OX/(4,2)MoS₂NTs) has metal behavior. For P impurity, which is used in different distance, the

behavior is changed from metal to semi-metal with direct transition at Z point. The behavior of this complex structure is became n-type semiconductor at 1.76 Å. For (OX/Ga-doped (4,2)MoS₂NTs) at different distance has a metal behavior, except the 1.82 Å has a n-type semiconductor behavior. The stability of this complex structure became more stable with Ga impurity and the Fermi level is shifted down compared others cases. The stability of all complex structures with Ga impurity is more stable compared with P impurity. Then, the greatest substrate of the (3,2) and (4,2) MoS₂NTs can be employed to career the OX anticancer drug when we utilized Ga impurity compared with P impurity.

Acknowledgements:

We are deeply appreciative of the provision of essential resources and facilities by University of Thi-Qar, College of Science, Department of Physics, which facilitated the smooth execution of our research activities. This research is part of master graduation requirements.

Copyright:

© 2024 by the authors. This article is an open access article distributed under the terms and conditions of the Creative Commons Attribution (CC BY) license (<https://creativecommons.org/licenses/by/4.0/>).

References

- [1] Piya, A.A., et al., *Adsorption behavior of cisplatin anticancer drug on the pristine, Al-and Ga-doped BN nanosheets: A comparative DFT study*. Computational and Theoretical Chemistry, 2021. **1200**: p. 113241.
- [2] Niyitanga, T., et al., *Carbon nanotubes-molybdenum disulfide composite for enhanced hydrogen evolution reaction*. Journal of Electroanalytical Chemistry, 2019. **845**: p. 39-47.
- [3] Yoshida, K., R. Yura, and Y. Nonoguchi, *Molecular electron doping to single-walled carbon nanotubes and molybdenum disulfide monolayers*. Nano Express, 2022. **3**(4): p. 044001.
- [4] Wu, X., et al., *Frontispiece: Covalently Aligned Molybdenum Disulfide–Carbon Nanotubes Heteroarchitecture for High-Performance Electrochemical Capacitors*. Angewandte Chemie International Edition, 2021. **60**(39).
- [5] Mohammed, M.H. and F.H. Hanoon, *Zinc oxide nanosheet as a carrier to various anticancer drugs delivery by utilizing DFT method*. Chinese Journal of Physics, 2022. **77**: p. 291-299.
- [6] Rezvani, M., et al., *Theoretical insights into the encapsulation of anticancer Oxaliplatin drug into single walled carbon nanotubes*. J Nanoanal, 2016. **3**(3): p. 69-75.
- [7] Mohammed, M.H. and F.H. Hanoon, *Bilayer MSe₂ and MS₂ (M= Mo, W) as a novel drug delivery system for β-lapachone anticancer drug: Quantum chemical study*. Computational and Theoretical Chemistry, 2020. **1190**: p. 112999.
- [8] Nafiu, S., et al., *Boron nitride nanotubes for curcumin delivery as an anticancer drug: a DFT investigation*. Applied Sciences, 2022. **12**(2): p. 879.
- [9] Nimr Ajeel, F., A. Mohsin Khuodhair, and S. Mahdi AbdulMohsin, *Improvement of the optoelectronic properties of organic molecules for nanoelectronics and solar cells applications: via DFT-B3LYP investigations*. Current Physical Chemistry, 2017. **7**(1): p. 39-46.
- [10] Hesabi, M. and R. Behjatmanesh-Ardakani, *Interaction between anti-cancer drug hydroxycarbamide and boron nitride nanotube: a long-range corrected DFT study*. Computational and Theoretical Chemistry, 2017. **1117**: p. 61-80
- [11] Ajeel, F.N., M.H. Mohammed, and A.M. Khudhair, *SWCNT as a model nanosensor for associated petroleum gas molecules: via DFT/B3LYP investigations*. Russian Journal of Physical Chemistry B, 2019. **13**: p. 196-204.
- [12] Ajeel, F.N., *Engineering electronic structure of a fullerene C₂₀ bowl with germanium impurities*. Chinese Journal of Physics, 2017. **55**(5): p. 2134-2143.
- [13] Khudhair, A.M., F.N. Ajeel, and M.H. Mohammed, *Theoretical (DFT and TDDFT) insights into the effect of polycyclic aromatic hydrocarbons on Monascus pigments and its implication as a photosensitizer for dye-sensitized solar cells*. Microelectronic Engineering, 2019. **212**: p. 21-26.
- [14] Khudhair, A.M., et al. *Enhancement the electronic and optical properties for the dye Disperse Orange 13 and using in the solar cell device*. in *IOP Conference Series: Materials Science and Engineering*. 2020. IOP Publishing.
- [15] Hommod, M.K. and L.F. Auqla, *Density Functional Theory Investigation For Ni6, Co5, Au12, Y5 and Ni6Li, Co5Li, Au12Li, Y5Na Interactions*. University of Thi-Qar Journal of Science, 2022. **9**(2): p. 105-112.
- [16] Mutier, M.N. and L.F. Al-Badry, *Effect of Direct Coupling on Electronic Transport and Thermoelectric Properties of Single Pyrene Molecule*. University of Thi-Qar Journal of Science, 2021. **8**(2): p. 94-99.
- [17] Ajeel, F.N., M.H. Mohammed, and A.M. Khudhair, *Effects of lithium impurities on electronic and optical properties of graphene nanoflakes: a DFT–TDDFT study*. Chinese Journal of Physics, 2019. **58**: p. 109-116.
- [18] Mohammed, M.H., B.A. Jarullah, and F.H. Hanoon, *Using of cellulose with various nanoparticles as chelating factors in nanovaccines: Density functional theory investigations*. Solid State Communications, 2020. **316**: p. 113945.

- [19] Mohammed, M.H. and F.H. Hanoon, *Zinc oxide nanosheet as a promising route for carrier 5-fluorouracil anticancer drug in the presence metal impurities: Insights from DFT calculations*. Computational and Theoretical Chemistry, 2021. **1194**: p. 113079.
- [20] Mohammed, M.H. and F.H. Hanoon, *Application of zinc oxide nanosheet in various anticancer drugs delivery: quantum chemical study*. Inorganic Chemistry Communications, 2021. **127**: p. 108522.
- [21] Odularu, A.T., P.A. Ajibade, and J.Z. Mbese, *Impact of molybdenum compounds as anticancer agents*. Bioinorganic chemistry and applications, 2019. **2019**.
- [22] Li, C., et al., *Bandgap engineering of monolayer MoS₂ under strain: A DFT study*. Journal of the Korean Physical Society, 2015. **66**: p. 1789-1793.
- [23] Wang, Z., et al., *Mixed low-dimensional nanomaterial: 2D ultranarrow MoS₂ inorganic nanoribbons encapsulated in quasi-1D carbon nanotubes*. Journal of the American Chemical Society, 2010. **132**(39): p. 13840-13847.
- [24] Yue, Q., et al., *Mechanical and electronic properties of monolayer MoS₂ under elastic strain*. Physics Letters A, 2012. **376**(12-13): p. 1166-1170.
- [25] Mohammed, M.H., A.S. Al-Asadi, and F.H. Hanoon, *Semi-metallic bilayer MS₂ (M= W, Mo) induced by Boron, Carbon, and Nitrogen impurities*. Solid State Communications, 2018. **282**: p. 28-32.